JMEPEG (2005) 14:163-172
DOI: 10.1361/10599490522338

©ASM International
1059-9495/$19.00

Time-Modulated Chemical Vapor Deposition of Diamond Films

M.J. Jackson, G.M. Robinson, W. Ahmed, H. Sein, A.N. Jones, N. Ali, E. Titus, Q.H. Fan, and J. Gracio

(Submitted August 31, 2004)

This article investigates the role of substrate temperature in the deposition of diamond films using a newly developed time-modulated chemical vapor deposition (TMCVD) process. TMCVD was used to deposit polycrystalline diamond coatings onto silicon substrates using hot-filament chemical vapor deposition system. In this investigation, the effect of (a) substrate temperature and (b) methane (CH_4) content in the reactor on diamond film deposition was studied. The distinctive feature of the TMCVD process is that it time-modulates CH_4 flow into the reactor during the complete growth process. It was noted that the substrate temperature fluctuated during the CH_4 modulations, and this significantly affected some key properties of the deposited films. Two sets of samples have been prepared, in each of which there was one sample that was prepared while the substrate temperature fluctuated and the other sample, which was deposited while maintaining the substrate temperature, was fixed. To keep the substrate temperature constant, the filament power was varied accordingly. In this article, the findings are discussed in terms of the CH_4 content in the reactor and the substrate temperature. It was found that secondary nucleation occurred during the high timed CH_4 modulations. The as-deposited films were characterized for morphology, diamond-C phase purity, hardness, and surface roughness using scanning electron microscopy, Raman spectroscopy, Vickers hardness testing, and surface profilometry, respectively.

Keywords biomedical applications, chemical vapor deposition, diamond films, thin films

1. Introduction

Diamond is a unique engineering material, due to its superior combination of physical, optical, and chemical properties (Ref 1, 2). As a result, the material has many potential uses in numerous industrial and consumer applications (Ref 3, 4). The difficulty in depositing truly superior diamond films is nearly as extreme as its unique properties. Researchers throughout the world have used a range of thin film-coating technologies to deposit diamond onto a range of substrate materials (Ref 5-7). However, the most successful method of deposition is chemical vapor deposition (CVD), because it yields films with a high degree of sp^3 bonding. It is generally accepted that the morphology, crystal size, crystal orientation, film quality, surface roughness, and coating adhesion are critical in determining the suitability of the coating being used for a particular application. It is essential to be able to design the coating to suit the specific application. Therefore, it is necessary to control film microstructure, morphology, and surface roughness, for example, to produce films that will display superior properties for new applications. Generally, CVD methods produce films that display rough surfaces, which become pronounced with the increase in film thickness. This limits their potential for use in mechanical, biomedical, and optical applications. It is highly desirable to be able to produce smooth films at reasonable growth rates. In addition, due to the nonuniform growth profile of the conventional CVD diamond films, intrinsic stresses are induced into the growing films during deposition (as high as 1 GPa). Intrinsic stresses are known to adversely affect a number of key thin film properties. Furthermore, the grain-to-grain-boundary ratio of the as-grown films changes along the depth of the film. This again brings about variations in film properties.

The most widely used method for producing low-roughness films is by polishing the deposited coatings after the film has been deposited. However, some difficulties arise during film polishing using standard polishing methods. As a result, techniques such as chemical mechanical polishing, and inert and oxygen ion-beam polishing have been developed to smooth the films after growth (Ref 8-11). In recent years, more controlled techniques, such as bias-enhanced nucleation and nanoparticle seeding have been used to deposit smoother films (Ref 12-14). Several researchers have tried pulse biasing during diamond CVD to produce highly orientated diamond films, using different pulse-bias duty cycles (Ref 15, 16). However, more detailed work is needed before the full potential of pulsed biasing can be realized. An in situ method, which consists of sequential in situ diamond deposition and planarization in an electron cyclotron resonance plasma system, has also been developed to produce smoother films (Ref 17). This method is believed to have the advantage of reducing processing time and costs, as well as maintaining a cleaner process environment. In addition to these methods, researchers have introduced trace amounts of gases, such as nitrogen, argon, and boron into the CVD reactor during deposition to alter the plasma characteristics to produce smoother films (Ref 18, 19).

Silva et al. (Ref 20) attempted to grow smooth diamond

M.J. Jackson and **G.M. Robinson,** Department of Mechanical Engineering Technology, Purdue University, West Lafayette, IN 47907-2021; **W. Ahmed, H. Sein,** and **A.N. Jones,** Department of Chemistry and Materials, Manchester Metropolitan University, Chester Street, Manchester, M1 5GD, U.K.; and **N. Ali, E. Titus, Q.H. Fan,** and **J. Gracio,** Department of Mechanical Engineering, University of Aveiro, 3810-193 Aveiro, Portugal. Contact e-mail: jacksonmj@purdue.edu.

films at lower temperatures by employing a two-step growth process. They proposed to promote non-diamond-phase nucleation onto (111) faces. However, no significant progress concerning the smoothness of the film was obtained. Difficulties were encountered in promoting secondary nucleation on a particular facet at low deposition temperatures (~550 °C). Secondary nucleation occurs more favorably on (111) and (100) diamond facets (Ref 21, 22). Instead, they proposed using a gold interlayer between two diamond layers to control the surface roughness. Chen and Hong (Ref 23) and Kumar et al. (Ref 24) used a two-step growth process that was similar to that used by Silva et al. (Ref 20) to produce diamond like carbon (C) films. These workers used such processes to control the stress and to improve the adhesion of the resultant films. In addition, smooth nanocrystalline diamond films have also been deposited using a range of methods (Ref 25-43).

Recently, a new time-modulated CVD (TMCVD) process for depositing smooth diamond films was reported (Ref 44). The key feature of the new process that differentiates it from other conventional CVD processes is that it pulses CH_4, at different concentrations, throughout the growth process, whereas, in conventional CVD, the CH_4 concentration is kept constant, for the full growth process, at one value. In TMCVD, it is expected that secondary nucleation processes occur during the stages of higher CH_4 concentration pulses. This can effectively result in the formation of a diamond film involving nucleation stage, diamond growth, secondary nucleation, and the cycle is repeated. The secondary nucleation phase can inhibit the further growth of diamond crystallites. The nuclei grow to a critical level and then are inhibited when secondary nuclei form on top of the growing crystals and fill up any surface irregularities. This methodology of diamond deposition presents a new regimen of film growth compared with the traditional columnar growth mode observed with conventional diamond CVD processes.

The process of dynamic film growth using CH_4 modulations constitutes an interesting concept in CVD diamond technology. The first article on TMCVD was published in 2002 (Ref 44). As a comparison, the process was also implemented for diamond growth using both hot-filament CVD and microwave CVD systems (Ref 45, 46). The authors then published the first article highlighting the role of substrate temperature in time-modulated diamond deposition (Ref 1). In this article, the authors discuss the TMCVD process in depositing diamond films. However, the TMCVD process is not yet fully understood; for example, the mechanisms involved during film growth remain uninvestigated.

2. Experimental

Diamond films were deposited onto silicon (Si) (100) substrates (5 × 5 × 0.5 mm). The substrates were abraded with diamond powder prior to film deposition to enhance the nucleation density. A conventional hot-filament CVD system (Ref 45) was used to deposit the diamond films. Prior to the depositions, the filament was precarburized to prevent filament poisoning. Before loading the samples in the CVD reactor, the substrates were ultrasonically cleaned in acetone for 10 min to remove any loose abrasive particles. In this investigation, four types of samples (samples A-D) were prepared. The conditions used during the growth of samples A to D are shown in Table 1. The variations in substrate temperature with CH_4 flow during the preparation of samples A to D are shown schematically in Fig. 1(a) to (d). The substrate temperature was measured using a K-type thermocouple, which was kept close to the substrate during deposition.

A scanning electron microscope (SEM) was used to characterize the films for morphology. A surface profiler was used to measure the surface roughness of the films. In addition, a micro-Raman system with a 632 nm helium-neon laser was used to characterize the diamond films for diamond-C-phase purity. The hardness of the coatings was measured using a Vickers hardness tester. The load applied during the hardness testing was 5 N for 20 s.

3. Results

Figure 2 displays SEM micrographs showing the surface morphologies of samples A, B, C, and D. It is evident that the four samples displayed different morphologies from one another. However, all the samples displayed good film uniformity and coverage. For simplicity, samples A and C, and samples B and D have been grouped, and from here onward these groups are referred to as set I and set II, respectively. In set I, the samples were prepared under conditions where the substrate temperature was fluctuated during the timed CH_4 modulations, whereas set II samples were prepared using TMCVD, under conditions where the substrate temperature was kept fixed, at a constant value, throughout the total number of timed CH_4 modulations. From the four samples, samples C and D consisted of smaller-sized diamond crystallites, where the average crystallite size was in the nanometer range. Although the average diamond crystallite size changed in each of the four samples, the crystal orientation was found to be predominantly (111).

Figure 3 displays the Raman sketches corresponding to the samples: (a) A, (b) B, (c) C, and (d) D. The diamond characteristic Raman peak, centered at 1332 cm^{-1}, was observed with all the samples except in the case of sample D. A broad band corresponding to the nondiamond impurities also appeared at around 1580 cm^{-1} in samples C and D. The slight broad band/shoulder observed in Fig. 3(a) disappeared in the Raman sketch for sample B. Generally, it was observed from the assessments

Table 1 Deposition conditions employed during preparation of samples A, B, C, and D

Sample	H_2 flow, sccm	CH_4 flow, sccm	CH_4 modulation times, min	Pressure, torr	Growth time, min	Substrate temperature, °C
A	150	4.5, 3	8, 10	30	126	776-802
B	150	4.5, 3	8, 10	30	126	802
C	150	6, 3	8, 10	30	126	760-802
D	150	6, 3	8, 10	30	126	802

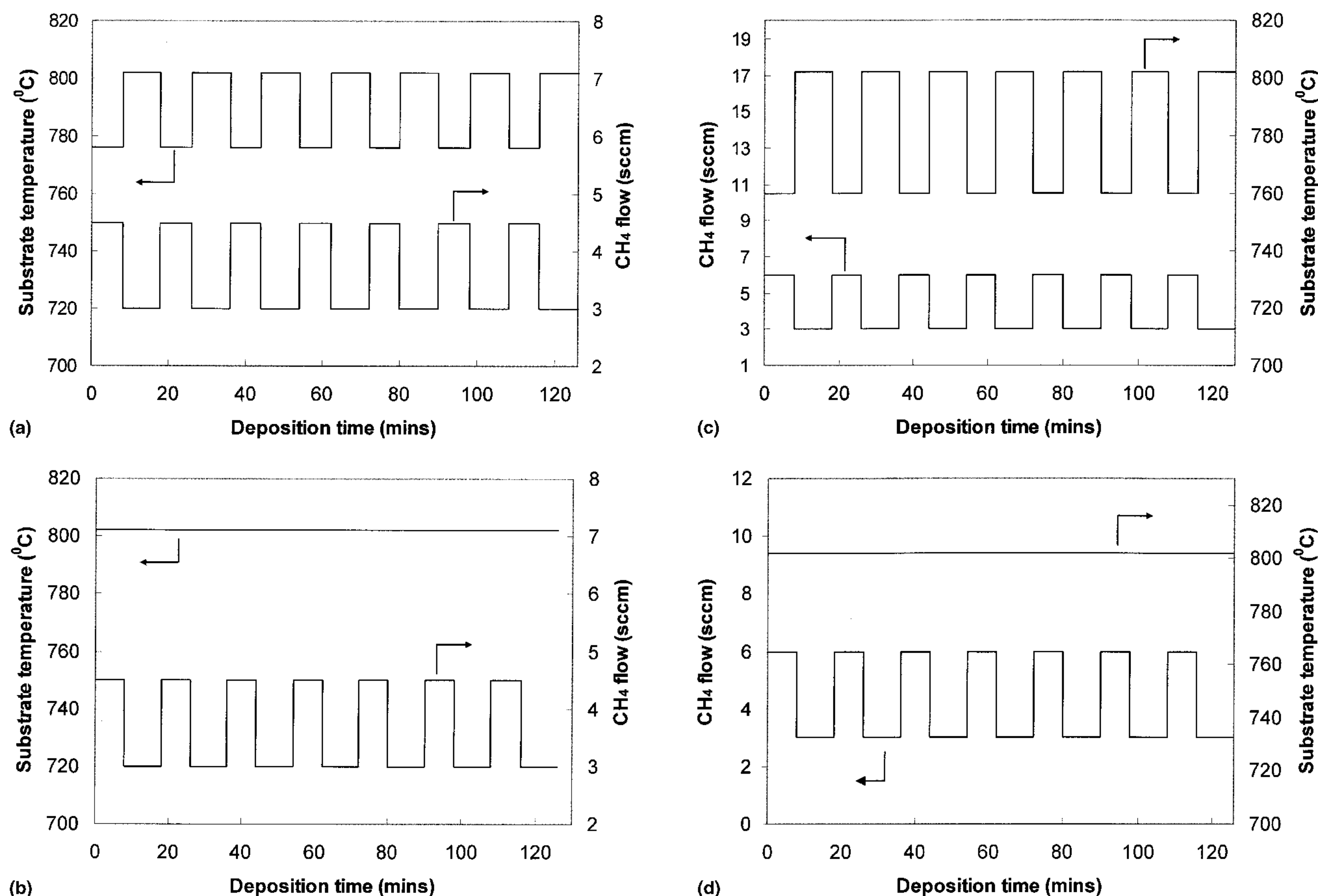

Fig. 1 Variations in substrate temperature and CH_4 flow during the TMCVD process for samples (a) A, (b) B, (c) C, and (d) D

of the intensities of the Raman diamond peaks and the nondiamond C-phase bands present on the Raman spectra that set I samples displayed better film quality.

The promotion of secondary nucleation during the high CH_4 modulations is an integral and distinctive feature of the TMCVD process. Figure 4 displays SEM micrographs showing secondary nucleation occurring after modulating CH_4 at 4.5 sccm (Fig. 4a) and 6 sccm (Fig. 4b) for 10 min. It is important to note that prior to the CH_4 pulses, diamond deposition was conducted under standard conditions (2% CH_4, constant flow) for 1 h using the hot filament chemical vapor deposition (HFCVD) system. The SEM images showed that secondary nucleation occurred, in both cases, during the CH_4 bursts at 4.5 and 6 sccm. However, the secondary nucleation density is greater after the CH_4 burst at 6 sccm than after that at 4.5 sccm. This can be expected, because at higher CH_4 concentrations C-containing radicals are present in the reactor in greater amounts, which favors the growth process by initiating diamond nucleation. The average secondary nucleation crystallite size was in the nanometer range. The SEM image shown in Fig. 4(b1) was magnified and was shown in Fig. 4(b2) to allow closer examination of the secondary nuclei. It is evident that the generation of secondary nucleation has led to the successful filling of the surface irregularities found on the film profile, between the mainly (111) crystals with these newly formed nanosized diamond grains. Figure 4(c) pictorially shows the consequence of modulating CH_4 on the production of secondary diamond crystallites on the surface of the diamond film. The surface roughness values of the two samples (in Fig. 4) were measured, and it was found that the 10 min CH_4 pulse at 6 sccm produced a smoother surface, giving rise to a surface roughness average (R_a) value of 0.25 μm, whereas the 10 min CH_4 burst at 4.5 sccm produced a less smooth film surface at an R_a value of 0.28 μm.

Figure 5(a) shows the growth rates for samples A to D. The growth rate values were generally higher for samples C and D than for samples A and B. The average growth rates for samples A, B, C, and D were found to be 0.70, 0.77, 1.20, and 1.58 μm/h, respectively. Figure 5(b) shows the graph representing the surface roughness of samples A to D. It can be seen that set II samples displayed relatively lower surface roughness values. The difference in the R_a values, as shown in Fig. 5(b), for samples A and B was 0.05 μm. Further, the difference in the R_a values for samples C and D was 0.11 μm. Figure 5(c) displays the graph showing the Vickers hardness data for samples A, B, C, and D. The variation in the data obtained with each of the four samples is shown on the graph in Fig. 5(c). A load of 500 g for 20 s was used to perform the indentations in assessing the hardness of the four samples. The average hardness values for samples A, B, C, and D were 685, 700, 840, and 1406 HV, respectively. The Vickers hardness values, displayed in Fig. 5(c), show a linear relationship, as was observed with

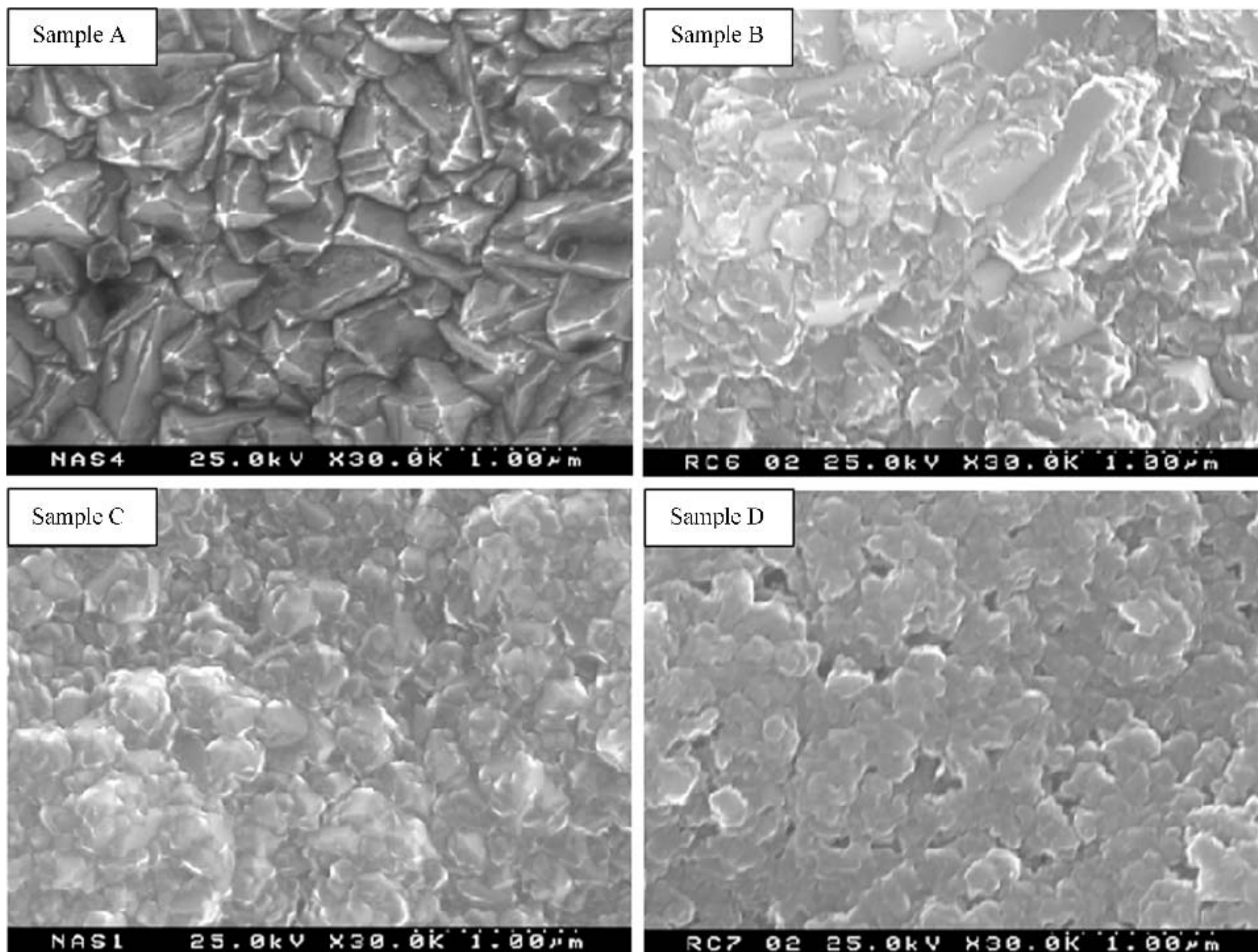

Fig. 2 SEM images showing the surface morphologies of samples A to D

the growth-rate results (Fig. 5a). After the indentations, the indented samples were closely examined using optical microscopy for any possible film delamination from the substrate. No such delamination was observed in all of the four samples tested, and the film coatings remained bonded to their respective silicon (Si) substrates. Si is a widely used substrate material for diamond deposition, and because it is a strong carbide-forming material good adhesion can be anticipated between the film coating and the Si.

A previous investigation (Ref 47) has demonstrated that the TMCVD process presents a different and new regimen of film growth compared with the traditional columnar growth mode observed with conventional diamond CVD processes. Because the distinctive feature of the TMCVD process is the timed CH_4 modulations, it was necessary and also timely to study the influence of such CH_4 modulations on the substrate temperature during film deposition. Substrate temperature is another critical parameter in diamond CVD, which influences key film properties.

Figure 6 displays the graph relating substrate temperature to CH_4 concentration (percent), in the vacuum chamber, under standard diamond CVD growth conditions. The influence of CH_4 concentration in the vacuum reactor, during film growth, was monitored at three different pressures: 10, 50, and 100 torr. Generally, the substrate temperature decreased with increasing CH_4 concentration. It should be noted that the observed temperature trend was obtained in the presence of two gases, namely, CH_4 and hydrogen, which were present in the reactor chamber during diamond CVD. Although the trend remained the same at the three different pressures (10, 50, and 100 torr), on increasing the deposition pressure the substrate temperature gradually decreased.

To monitor the changes in the substrate temperature when the flow of CH_4 into the chamber is stopped, at a certain point in the growth process an experiment was performed in which the CH_4 flow was terminated at a certain point while maintaining the constant, steady flow of hydrogen gas (Fig. 7). Two sets of experimental runs were conducted to study the influence of CH_4 concentration in the reactor chamber on the substrate temperature. Prior to CH_4 termination, the reactor consisted of 2% and 3% CH_4, then subsequently in each of the two cases the CH_4 flow into the reactor was terminated, and the substrate temperature was measured while the reactor pressure was (a) kept constant (Fig. 7a) and (b) not kept constant (Fig. 7b). In Fig. 7(a), it is worth noting that the pressure in the reactor chamber was kept constant, at 30 torr, throughout this experiment. It is interesting to note that the substrate temperature increased exponentially and reached a steady state after approximately 60 s (Fig. 7a). It is clear from Fig. 7(a) that the final measured temperature was the same in both of the experimental runs, and that at this point the CH_4 had been evacuated from the reactor and from here onward only hydrogen

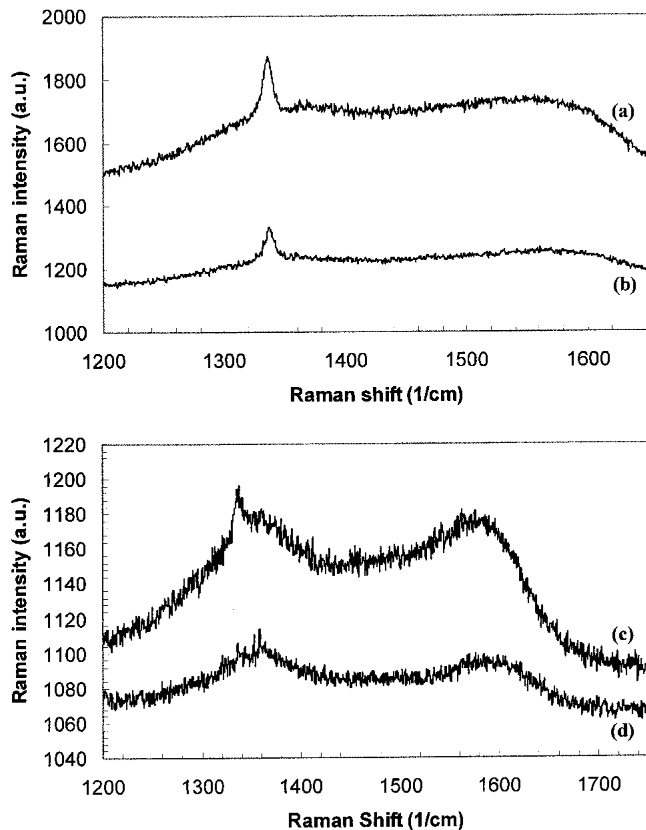

Fig. 3 Raman spectra of samples (a) A, (b) B, (c) C, and (d) D

plasma existed in the vacuum chamber. It can be seen from both graphs in Fig. 7(a) and (b) that the substrate temperature, at the beginning of the experiment, was noted to be relatively high for lower CH_4 concentrations. Figure 7(b) shows the substrate temperature results obtained when the pressure was not kept constant. Therefore, as the CH_4 molecules were being pumped out of the reactor, the pressure in the chamber decreased, as expected. When initially there was 2% CH_4 in the reactor at 30 torr pressure, prior to CH_4 flow termination, the final pressure noted at the end of the experiment was 25 torr. However, when the initial CH_4 concentration was 3% at 30 torr pressure, the final pressure noted was 22 torr. Due to this 3 torr difference in the final pressure reading, which alters the mean-free-path (MFP) values of species in the reactor, there is a difference in the steady-state temperature observed in both cases. The final temperature values, noted after the complete evacuation of CH_4 from the chamber, when the initial CH_4 concentration was 2 and 3% were 870 and 877 °C, respectively. Therefore, the difference of 7 °C in the substrate temperature corresponds to the 3 torr difference in reactor pressure, which was noted.

To investigate the independent effect of CH_4 on the substrate temperature, only CH_4, without any hydrogen flow, was introduced into the vacuum chamber and the substrate temperature was measured. Figure 8 shows that the substrate temperature remained almost constant, at around 730 °C, with varying CH_4 flow at 25 torr pressure. The experiment was also repeated for only hydrogen flow and no CH_4 in the chamber (Fig. 9). Once again, the substrate temperature remained constant, at a value of approximately 810 °C, with the H_2 flow rate. The pressure was maintained at 30 torr at the different H_2 flow rates. The flow rate used in this experiment for H_2 gas was increased from 50 to 200 sccm in 50 sccm increments.

The variation in the substrate temperature with timed CH_4 modulations can be noticed from Fig. 10. Two CH_4 flow values were used in this experiment, 4.5 and 3 sccm, which represent 3 and 2% of CH_4 in the vacuum reactor, respectively. At 4.5 and 3 sccm CH_4 flows, the substrate temperatures recorded were 811 and 827 °C, respectively. In modulating the CH_4 flow from 4.5 to 3 sccm and vice versa (i.e., one modulation cycle), the average stabilization time required was approximately 35 to 40 s. As the CH_4 flow was reduced from 4.5 to 3 sccm, the substrate temperature increased steadily and then stabilized to a constant value. The steady temperature was attained only after the CH_4 reached a steady-state value.

In preparing film samples in set II, the substrate temperature was kept constant during the CH_4 modulation cycles by adjusting the filament power accordingly. Figure 11 displays the graph showing the relationship between filament power (Watts) and CH_4 flow (sccm) to keep the substrate temperature at 800 °C. Generally, as the CH_4 content increased in the chamber at 30 torr pressure, more power was required to maintained the 800 °C substrate temperature. At 1.5 sccm CH_4 flow, the filament power required to maintain the target temperature was approximately 193 W, whereas, at 7.5 sccm CH_4 flow, the filament power used was 256 W.

4. Discussion

Again for simplicity, samples were prepared in which the substrate temperature fluctuated during the CH_4 modulation cycles (samples A and C), which from here onward are referred to as temperature-fluctuated films (TFFs), whereas samples prepared under constant substrate temperature (samples B and D) are referred to as temperature-controlled films (TCFs). Furthermore, from this point onward, samples A and B are labeled as set A, and samples C and D as set B. The principal difference in preparing set A and B is the different CH_4 flow rates used during the depositions. Set A samples were prepared using lower flows of CH_4, whereas, set B samples were deposited using relatively higher CH_4 flows, as shown in Fig. 1.

In discussing the results of this investigation, it is reasonable to attribute the experimental observations and findings related to the morphological changes together with the variation in the film properties displayed by TFF and TCF to two possible factors, namely, (1) the concentration of CH_4 in the vacuum reactor and (2) the substrate temperature during film deposition. The results of this study are discussed with respect to these two factors.

4.1 CH_4 Concentration

Because the CH_4 flow into the CVD reactor is modulated during film deposition, it is important to have an understanding about the quantity of C-containing species reaching the substrate surface, where the effective chemical vapor reactions take place to deposit the solid film. The number of molecules colliding on the surface of the substrate (S_n), Knudsen flow, per unit area, per unit time can be written as:

$$S_n = \frac{1}{4} P\,(\nu) \quad \text{(Eq 1)}$$

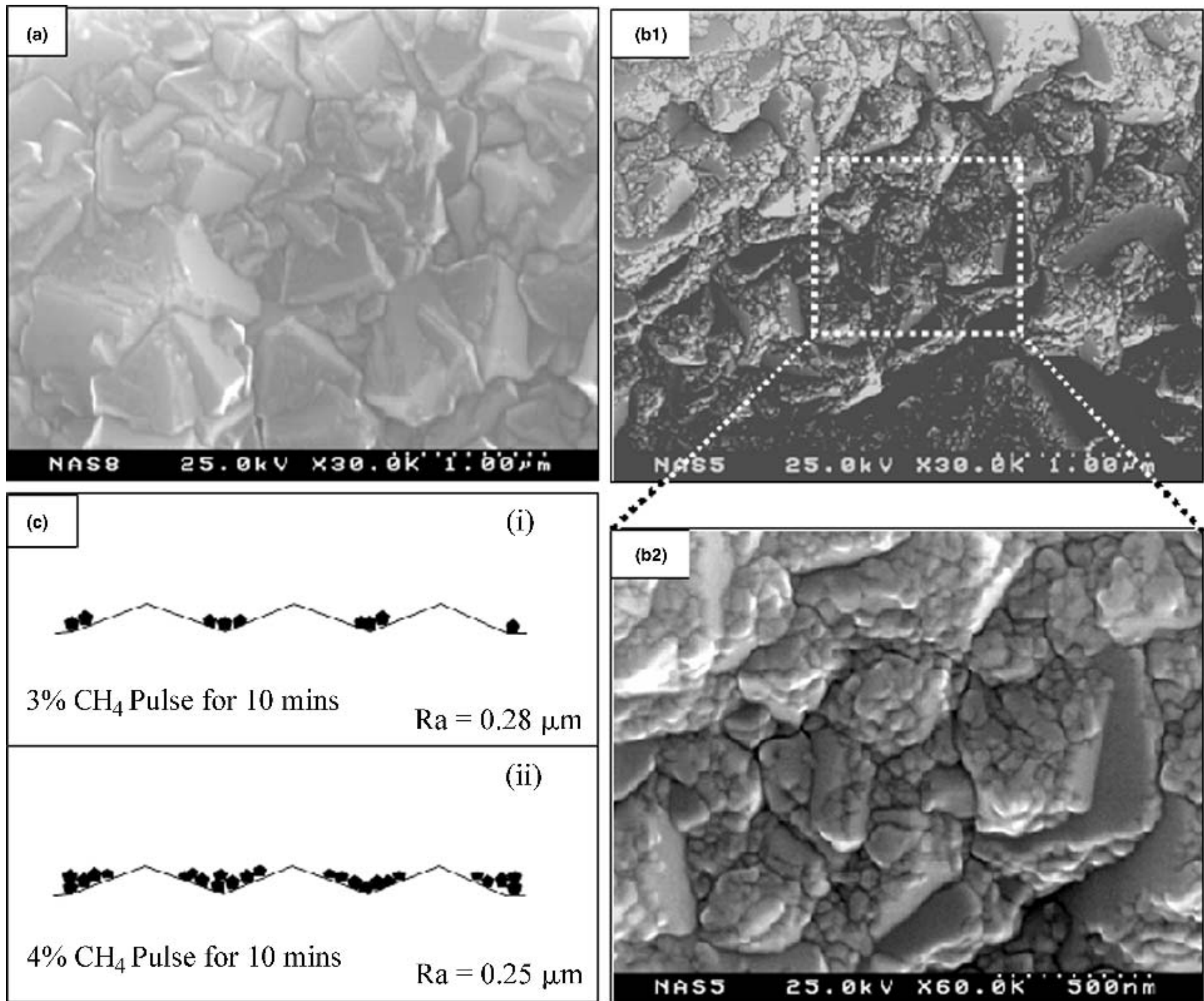

Fig. 4 SEM micrographs showing secondary nucleation occurring after modulating CH_4 at (a) 4.5 sccm and (b) 6 sccm for 10 min. (b2) is the magnified view of image (b1). (c) is the pictorial representation of the consequence of modulating CH_4 on the production of secondary diamond crystallites on the surface of the diamond films

where P is the pressure and (v) is the velocity of the molecules. The MFP of the molecule, λ, is given by:

$$\lambda = \frac{1}{\sqrt{2}\,\pi d^2 P} \quad \text{(Eq 2)}$$

where d is the diameter of the gas molecule. Substituting for P into Eq 1 gives:

$$S_n = \frac{(\nu)}{4\sqrt{2}\,\pi d^2 \lambda} \quad \text{(Eq 3)}$$

From Eq 3, it can de deduced that the number of molecules striking the substrate surface is inversely proportional to the MFP. It can be deduced from Eq 2 that the MFP is inversely proportional to the diameter of the molecule. The modulation of CH_4 from a low flow to a high flow will reduce the MFP (Eq 2), and, therefore, there will be an increase in the number of molecules striking the substrate. This will effectively lead to the formation of high-density diamond particle nucleation. Therefore, in set B, it is expected that at the higher CH_4 bursts, the number of C-containing radicals arriving at the substrate surface will be high compared with those in set A. Also, the MFP value will be lower, during the higher CH_4 bursts, and, therefore, there will be more collisions with more C-containing plasma species, which results in the generation of more diamond grains leading to higher nucleation processes occurring during the growth process. It has been shown (Ref 48) that the TMCVD process is very effective and efficient in increasing the homogeneous nucleation density of diamond crystallites on cemented tungsten carbide (WC-Co) substrates.

Raman spectroscopy showed that the film quality, in terms of diamond-C-phase purity, of set A samples was better than that of set B samples. It should be noted that the total flow of CH_4 into the vacuum chamber during the growth process was higher for depositing set B samples than for depositing set A samples. The presence of increased an quantity of CH_4 in the CVD reactor generally has an adverse effect on the global film quality (Ref 49). It is interesting to note that the slight shoulder appearing at around 1580 cm^{-1} for sample A almost disappeared in sample B. This suggests that the degree of nondia-

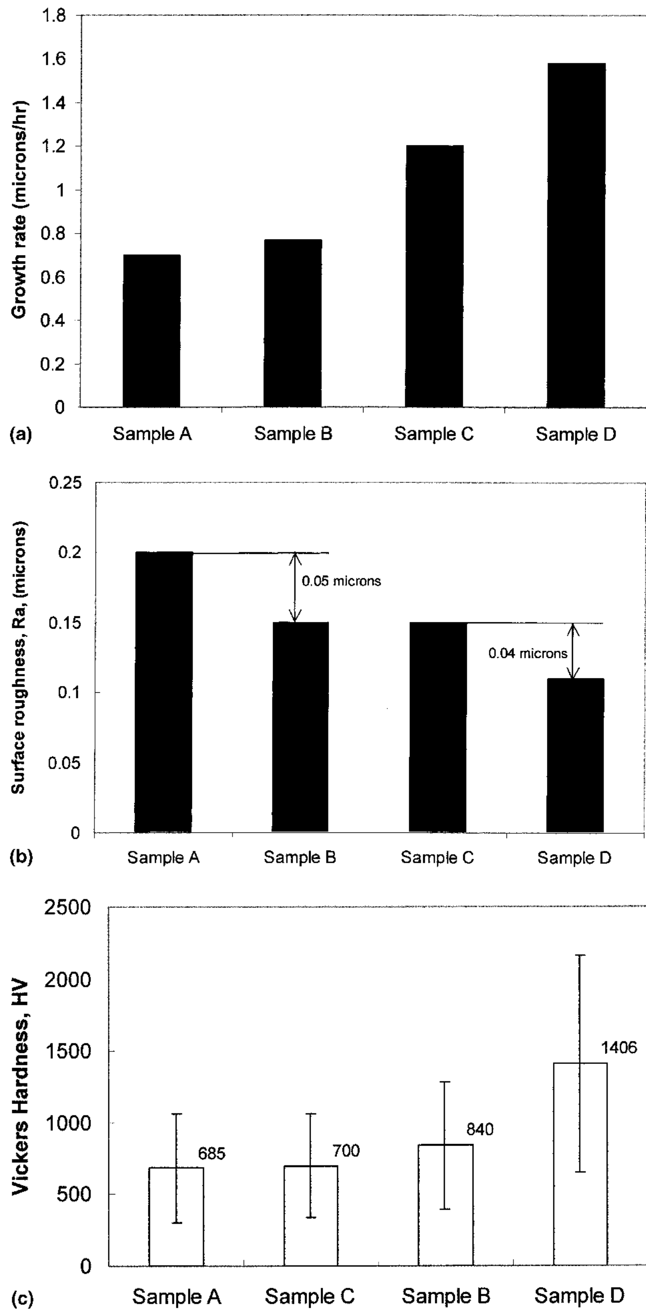

Fig. 5 Graphs showing the (a) growth rate, (b) surface roughness, and (c) Vickers hardness values for samples A to D

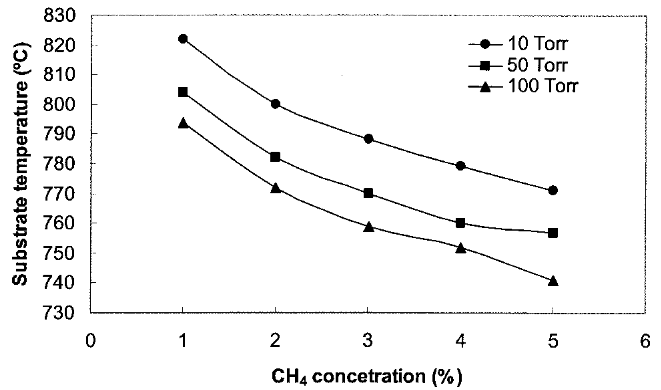

Fig. 6 Graph relating substrate temperature to CH_4 concentration (percent) in the vacuum chamber under normal diamond CVD growth conditions. Readings were taken for three pressures: 30, 50, and 100 torr

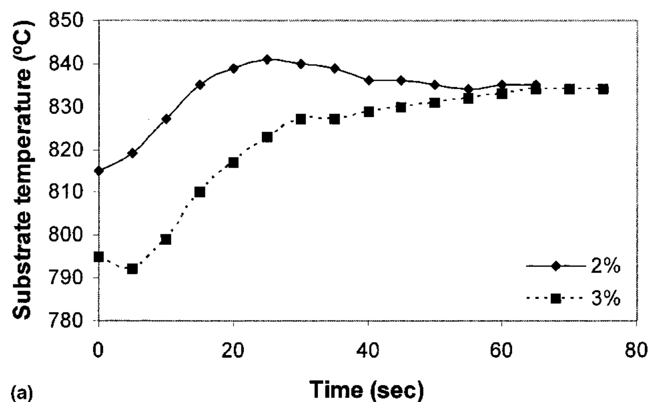

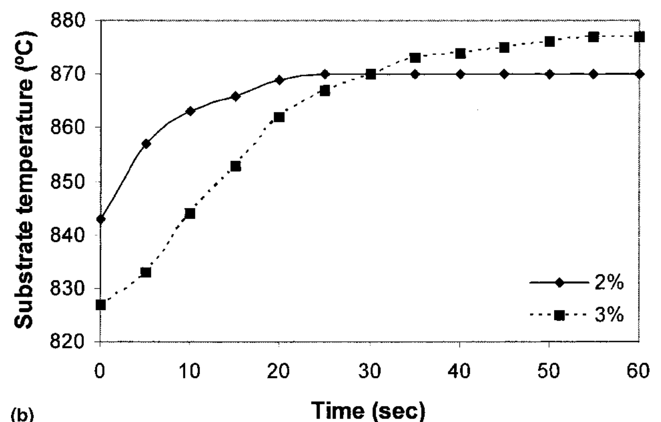

Fig. 7 Graph showing the variation in substrate temperature, once CH_4 is terminated and the hydrogen flow is kept constant. In (a) the reactor pressure was kept constant, and in (b) the pressure was not kept constant.

mond C phases in sample B decreased in magnitude compared with the non-diamond-phase levels in sample A. The SEM analysis and the Raman results support the authors' claims concerning the superiority of the film quality of sample A to that of sample B. Although there is a slight broad band emerging at around 1580 cm^{-1} for set B samples, the intensity of the characteristic Raman diamond peak was greater compared with the broad band. It is known that the Raman scattering coefficient is significantly higher for graphitic phases than for diamond phases (Ref 50). Thus, even very small concentrations of sp^2 phase could be easily detected using Raman spectroscopy. This implies that in set B, where the samples display the broad graphitic peaks, the overall quality of the film samples can be expected to be reasonably good.

The higher growth rates in set B are also due to the increased flow of CH_4 into the reactor. It is known that higher CH_4 content in the vacuum reactor results in increased growth rates. Furthermore, according to Eq 3 the number of molecules striking the substrate surface is higher at higher CH_4 concentration, which also lowers the MFP value. The effect of CH_4 concentration on growth rate can be explained by using Eq 1 to 3. The TCF samples displayed surface profiles that were relatively smooth compared with their corresponding TFF samples.

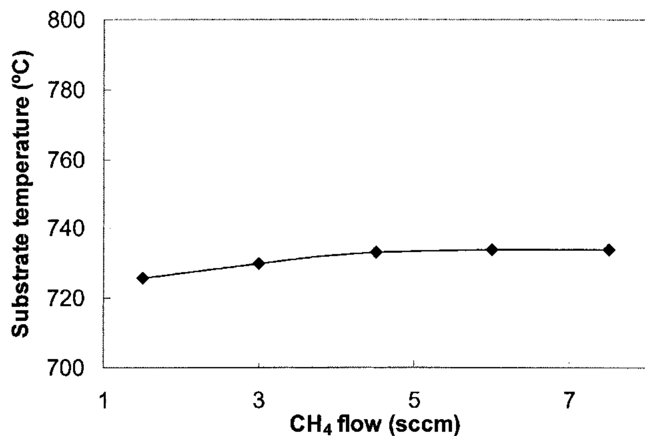

Fig. 8 Graph showing the variation in substrate temperature, when only CH_4 is present in the chamber. The pressure was kept constant at 25 torr.

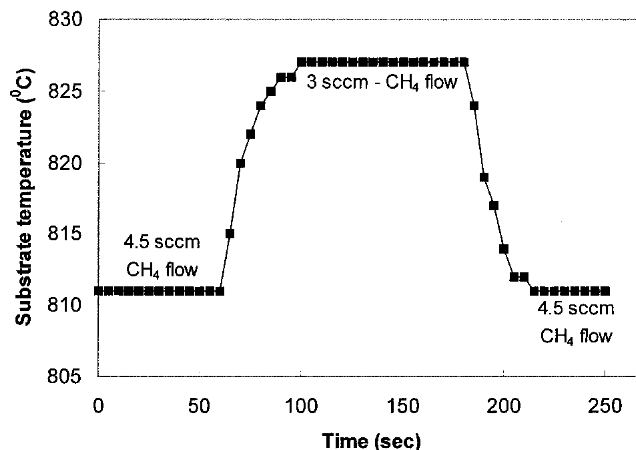

Fig. 10 Variation in the substrate temperature during a single timed CH_4 modulation

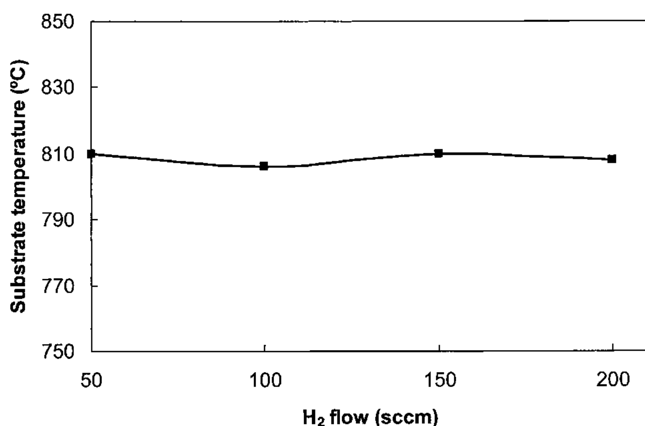

Fig. 9 Graph showing the variation in substrate temperature, when only hydrogen was present in the chamber. The chamber pressure was kept constant at 30 torr.

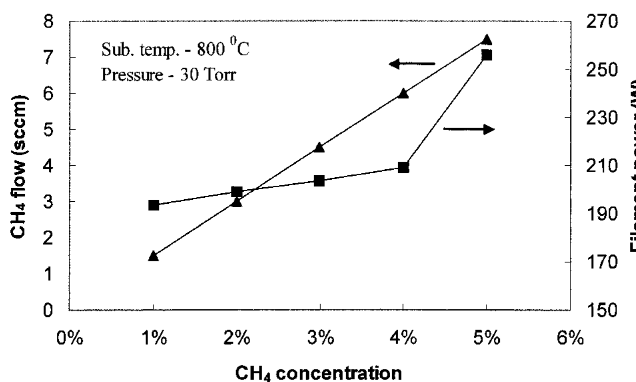

Fig. 11 Graph showing the relationships among CH_4 flow (sccm), CH_4 concentration (percent), and filament power (watts)

This is related to the secondary nucleation, as depicted in Fig. 4, which takes place during the high CH_4 modulations and is dependent on three parameters: (a) pressure, (b) temperature, and (c) CH_4 concentration. Figure 4 justifies the profound influence of CH_4 concentration on secondary diamond crystallite nucleation during the TMCVD process. The increased secondary nucleation density leads to the production of nanosized diamond crystallites. According to the classic nucleation theory (Ref 51) for spherical or cubic crystallites:

$$\text{Secondary nucleation rate } (\text{cm}^{-2}\,\text{s}^{-1}) = \frac{\text{growth rate } (\text{cm} \cdot \text{s}^{-1})}{\text{crystal size}} \quad \text{(Eq 4)}$$

The growth rate of diamond films deposited using CVD method is profoundly influenced by three parameters: (a) CH_4 concentration, (b) substrate temperature, and (c) deposition pressure. In this case, only parameters (a) and (b) were changed during the TMCVD process, and the pressure was kept constant during TFF and TCF depositions. Generally, it is known that the growth rate increases with CH_4 concentration, pressure, and substrate temperature. The influence of temperature on diamond film deposition in TMCVD is discussed in the next section.

The relationship in Eq 4 shows that as the growth rate increases and the crystallite size decreases, the secondary nucleation rate increases. The above relationship can be used to explain the results obtained in this study relating to surface morphology, crystallinity, surface roughness, and secondary nucleation rates. The findings in this research are consistent with Eq 4. The Vickers hardness tests displayed higher values for TCF samples than for their counterpart TFF samples. It is known that the hardness of a polycrystalline material is inversely proportional to its average grain size. Therefore, the smaller the grain size in the polycrystalline film, the higher the Vickers hardness value for that material.

4.2. Substrate Temperature

In TMCVD, the fluctuations in the substrate temperature during the timed CH_4 modulations need to be considered, because substrate temperature is a critical parameter having a significant influence on the diamond CVD process. There are

three main factors that can contribute to the substrate temperature changes observed during CH_4 modulations: (a) gas species thermal motion, (b) chemical reactions between C-containing species and hydrogen, and (c) the C-phase transitions. It is important to realize that generally during diamond CVD, these three factors come into play simultaneously.

According to the kinetic theory of gases, the average speed of the molecule is directly proportional to the temperature:

$$\langle v \rangle = \sqrt{\frac{8kT}{\pi m}} \qquad \text{(Eq 5)}$$

In hot-filament CVD, CH_4 and H_2 decompose at or near the filament surface and, consequently, form hydrogen-terminated methyl radicals. These C-containing radicals travel a certain distance to reach the substrate. The hydrogen-terminated methyl radicals may be traveling with a certain velocity (i.e., with kinetic energy attained from the filament temperature) and may impinge on the substrate surface. Therefore, at high filament power, the molecules travel with greater velocity, and the temperature of the substrate is directly related to the kinetic motion of the gas. At constant pressure, the speed of the molecule is directly related to the filament temperature. However, before discussing the effects of filament power on the film-growth process, it was noticed that the substrate temperature also depends on the nature of the reactive gas present inside the CVD reactor. When the CVD reactor contained both CH_4 and H_2, the temperature decreased with increasing CH_4 concentration. The decrease in substrate temperature (Fig. 5) with CH_4 concentration is due to the higher reaction rate of CH_4 with the dissociated hydrogen (endothermic reaction). Therefore, more C-species reach the substrate and condense on the surface to form the diamond grains. The condensation of the C-plasma species onto the surface to nucleate into diamond particles is considered to be a cooling process; therefore, the substrate temperature drops with increased CH_4 content. The increase in the substrate temperature, shown in Fig. 7(a) and (b), is due to the relatively low reaction rate between the atomic hydrogen and methyl radicals. The temperature remained steady when there was no CH_4 in the chamber. This is to be expected because enthalpy changes only when there are reactive species in the CVD reactor. When the vacuum chamber contains either CH_4 or H_2 alone (Fig. 8, 9), the dissociation and formation of CH_4 molecules is in equilibrium. Therefore, there is no enthalpy change, and the substrate temperature remains constant.

In performing a single timed CH_4 modulation, as part of the TMCVD process, it takes some time for the temperature to reach a constant value (Fig. 10). There is no sharp or abrupt rise in the substrate temperature, as seen in Fig. 10. The temperature remained steady only after the CH_4 concentration had reached a constant value.

It needs to be noted that the substrate temperature was kept constant in preparing TCF samples by accordingly adjusting the filament power. It was found that the filament power increased almost linearly (Fig. 11) with CH_4 flow and concentration in the vacuum chamber, at 30 torr pressure, to maintain the target 800 °C substrate temperature.

During the deposition of TCF samples in sets A and B, the substrate temperature was kept constant during the high CH_4 flow rates by increasing the filament power. Increasing the filament power at a higher CH_4 content in the reactor also increases the following parameters: (a) gas temperature close to the filament, (b) MFP, (c) atomic hydrogen, (d) ionization rate, and (e) electron emission current. Although an expression for MFP (λ) was used in Eq 2, MFP is also directly related to the temperature; therefore, Eq 6 can be used to explain the affect of temperature on λ:

$$\lambda = \frac{RT}{N_A P \pi \sigma^2 \sqrt{2}} \qquad \text{(Eq 6)}$$

where R is the universal gas constant, T is the temperature of the molecule, and N_A is Avogadro's constant. In accordance with Eq 6, as the filament power is increased at high CH_4 flow modulations during the deposition of TCF samples, the MFP increases. Due to this, the gas temperature increased too, and it can be expected that the molecules will travel with a greater velocity (Eq 5) and reach the substrate more rapidly. When this begins to happen, the flux of C-containing species rushes to the substrate where an increased number of effective reactions takes place. In the case of TCF in set B, the substrate surface becomes saturated with C-containing species. As a result more nanosized diamond crystallites are produced, and this also reduces the presence of the diamond C phase in the depositing film. The increase in the filament power results in an increase in the electron emission current, which increases the ionization rate. The increased ionization rate enables the production of a greater quantity of atomic hydrogen.

It is worth noting that hydrogen ions are very important in contributing significantly to the overall quality of the depositing films, because atomic hydrogen etches graphitic phases more favorably than etching diamond phases. During the deposition of TCF samples in sets A and B, it can be stated that the concentration of atomic hydrogen in the CVD reactor was greater compared with the concentration of hydrogen in the reactor during the deposition of TFF samples in sets A and B. Due to the increased etching of the nondiamond phases present in the TCF samples, the TCF samples contained relatively less sp^2 C.

The other main factor mentioned earlier, C-phase transition, occurring during diamond CVD also has a significant influence on the growth properties of diamond films. During diamond CVD, sp^3 C bonds appear under metastable conditions. The transition from sp^2 bond to sp^3 and/or from sp bond to sp^3 requires a large amount of localized energy (not under thermal equilibrium). This phenomenon can potentially lead to a decrease in the substrate temperature. Some researchers have shown that the growth of diamond on a nondiamond substrate is not a single-step process (Ref 52). Direct evidence for the formation of graphite on the substrates prior to diamond nucleation has been reported (Ref 53). It was found that the graphite film, formed initially on the substrate surface, greatly enhanced diamond nucleation (Ref 54). The high-resolution transmission electron microscopy (TEM) study of nucleation and the growth of diamond on copper TEM grids in HFCVD by Singh et al. (Ref 55) provided direct evidence for the formation of a diamondlike amorphous C layer, 8 to 14 nm thick, in which small diamond nanocrystallites, approximately 2 to 5 nm in size, were embedded, and large diamond crystallites were observed to grow from these nanocrystallites. It has been suggested (Ref 55) that nanocrystalline diamond grains were formed as a result of the direct transformation of the amorphous carbon into diamond, with the intermediate layer providing nucleation sites.

5. Conclusions

Polycrystalline diamond films were deposited onto Si substrates using the new TMCVD process. In this investigation, the influence of two parameters has been studied: (a) CH_4 concentration and (b) substrate temperature on diamond deposition using timed CH_4 modulations. For comparison, four types of samples were deposited. The TFF samples were deposited where the substrate temperature fluctuated during film growth. However, in depositing the TCF samples, the substrate temperature was kept constant throughout the growth process. Filament power was adjusted, accordingly, to stabilize the substrate temperature during the high and low CH_4 modulations. The variations in the CH_4 content and the substrate temperature were discussed in relation to a number of factors, including, for example, MFP and thermal gas velocities. The findings strengthen the understanding of the TMCVD process when used to deposit diamond films.

References

1. N. Ali, Y. Kousar, Q.H. Fan, V.F. Neto, and J. Gracio, *J. Mater. Sci. Lett.,* Vol 22, 2003, p 1039
2. P.W. May, *Philos. Trans. R. Soc. London, Ser. A*, Vol 358, 2000, p 473
3. M.N. Ashfold, P.W. May, C.A. Rego, and N.M. Everitt, *Chem. Soc. Rev.,* Vol 23, 1994, p 2
4. N. Ali, W. Ahmed, I.U. Hassan, and C.A. Rego, *Surf. Eng.,* Vol 14 (No. 4), 1998, p 292
5. H. Chen, M.L. Nielsen, C.J. Gold, R.O. Dillon, J. DiGregorio, and T. Furtak, *Thin Solid Films,* Vol 212, 1992, p 169
6. J.T. Huang, W.Y. Yeh, J. Hwang, and H. Chang, *Thin Solid Films,* Vol 315, 1998, p 35
7. Q.H. Fan, E. Pereira, and J. Gracio, *J. Mater. Sci.,* Vol 34, 1999, p 1353
8. C. Tokura, F. Yang, and H. Yoshikawa, *Thin Solid Films,* Vol 212, 1992, p 49
9. T. Zhao, D.F. Grogan, B.G. Bovard, and H.A. Macleod, *Appl. Opt.,* Vol 31, 1992, p 1483
10. A. Hirata, H. Tokura, and M. Yoshikawa, *Thin Solid Films,* Vol 212, 1992, p 43
11. D.G. Lee and R.K. Singh, in *Beam-Solid Interactions for Materials Synthesis and Characterization,* D.E. Luzzi, T.F. Heinz, M. Iwaki, and D.C. Jacobson, Ed., Materials Research Society, Symposium Proceedings No. 354, Pittsburgh, PA, 1995, p 699
12. I. Gouzman and A. Hoffman, *Diamond Relat. Mater.,* Vol 7, 1998, p 210
13. X. Li, Y. Hayashi, and S. Nishino, *Jpn. J. Phys.,* Vol 36, 1997, p 5197
14. H. Makita, K. Nishimura, N. Jiang, A. Hatta, T. Ito, and A. Hiraki, *Thin Solid Films,* Vol 281, 1996, p 279
15. S.D. Wolter, F. Okuzumi, J.T. Prater, and Z. Siter, *Phys. Status Solidi A,* Vol 186 (No. 2), 2001, p 331
16. B.D. Beake, I.U. Hassan, C.A. Rego, and W. Ahmed, *Diamond Relat. Mater.,* Vol 9, 2000, p 1421
17. D.R. Gilbert, D.-G Leeand, and K. Singh, *J. Mater. Res.,* Vol 13 (No. 7), 1998, p 1735
18. A.J. Eccles, T.A. Steele, A. Afzal, C.A. Rego, W. Ahmed, P.W. May, and S.M. Leeds, *Thin Solid Films,* Vol 343-344, 1999, p 627
19. A. Afzal, C.A. Rego, W. Ahmed, and R.I. Cherry, *Diamond Relat. Mater.,* Vol 7, 1998, p 1033
20. F. Silva, A. Gicquel, A. Chiron, and J. Achard, *Diamond Relat. Mater.,* Vol 9, 2000, p 1965
21. A. Gicquel, K. Hassouni, and F. Silva, *J. Electrochem. Soc.,* Vol 14716, 2000, p 2218
22. W. Zhu, A.R. Badzian, and R. Messier, *Diamond Opt*. Vol 111, 1990, p 187
23. C.F. Chen and T.M. Hong, *Surf. Coat. Technol.,* Vol 5, 1993, p 143
24. S. Kumar, P.N. Dixit, D. Sarangi, and R. Bhattacharyya, *J. Appl. Phys.,* Vol 85, 1999, p 3866
25. D.M. Bhusari, J.R. Yang, T.Y. Wang, K.H. Chen, S.T. Lin, and L.C. Chen, *J. Mater. Res.,* Vol 13 (No. 7), 1998, p 1769-1773
26. J. Michler, S. Laufer, H. Seehofer, E. Blank, R. Haubner, and B. Lux, "Chemical Vapor Diamond Deposition of Coatings," *Proc. 10th Int. Conf. on Diamond and Diamond-like Materials* (Prague, Czech Republic), Sept 1999, paper 5.231
27. D.M. Gruen, L. Shengzhong, A.R. Krauss, J. Luo, and X. Pan, *Appl. Phys. Lett.,* Vol 64 (No. 12), 1994, p 1502
28. D. Zhou, T.G. McCauley, L.C. Qin, A.R. Krauss, and D.M. Gruen, *J. Appl. Phys.,* Vol 83 (No. 1), 1998, p 540
29. D.M. Gruen, *Ann. Rev. Mater. Sci.,* Vol 29, 1999, p 211
30. T.M. McCauley, D.M. Gruen, and A.R. Krauss, *Appl. Phys. Lett.,* Vol 73 (No. 12), 1998, p 1646
31. D. Zhou, A.R. Krauss, L.C. Qin, T.G. McCauley, D.M. Gruen, T.D. Corrigan, R.P.H. Chang, and H. Gnaser, *J. Appl. Phys.,* Vol 82 (No. 9), 1997, p 4546
32. Y.F. Zhang, F. Zhang, Q.J. Gao, X.F. Peng, and Z.D. Lin, *Diamond Relat. Mater.,* Vol 10, 2001, p 1523
33. X.S. Sun, N. Wang, W.J. Zhang, H.K. Woo, X.D. Han, I. Bello, C.S. Lee, and S.T. Lee, *J. Mater. Res.,* Vol 14 (No. 8), 1999, p 3204
34. D.M. Bhusari, J.R. Yang, TY. Wang, K.H. Chen, S.T. Lin, and L.C. Chen, *Mater. Lett.,* Vol 36, 1998, p 279
35. H. Yagi, T. Ide, H. Toyota, and Y. Mori, *J. Mater. Res.,* Vol 13 (No. 6), 1998, p 1724
36. J. Lee, B. Hong, R. Messier, and R.W. Collins, *Appl. Phys. Lett.,* Vol 69 (No. 12), 1996, p 1716
37. T. Xu, S. Yang, J. Lu, Q. Xue, J. Li, W. Guo, and Y. Sun, *Diamond Relat. Mater.,* Vol 10, 2001, p 1441
38. S.P. McGinnis, M.A. Kelly, S.B. Hagstrom, and R.L. Alvis, *J. Appl. Phys.,* Vol 79 (No. 1), 1996, p 170
39. H. Yoshikawa, C. Morel, and Y. Koga, *Diamond Relat. Mater.,* Vol 10, 2001, p 1588
40. L.C. Chen, P.D. Kichambare, K.H. Chen, J.-J. Wu, J.R. Yang, and S.T. Lin, *J. Appl. Phys.,* Vol 89 (No. 1), 2001, p 753
41. S. Mitura, A. Mitura, P. Niedzielski, and P. Couvrat, *Chaos Solit. Fract.,* Vol 10 (No. 12), 1999, p 2165
42. T. Sharda, M. Umeno, T. Soga, and T. Jimbo, *Appl. Phys. Lett.,* Vol 77 (No. 26), 2000, p 4304
43. H. Yusa, *Diamond Relat. Mater.,* Vol 11, 2002, p 88
44. Q.H. Fan, N. Ali, W. Ahmed, Y. Kousar, and J. Gracio, *J. Mater. Res.,* Vol 17 (No. 7), 2002, p 1563
45. N. Ali, V.F. Neto, and J. Gracio, *J. Mater. Res.,* Vol 18 (No. 2), 2003, p 296
46. N. Ali, Q.H. Fan, Y. Kousar, W. Ahmed, and J. Gracio, *Vacuum,* Vol 71 (No. 4), 2003, p 445
47. N. Ali, V.F. Neto, Y. Kousar, G. Cabral, and J. Gracio, *Mater. Sci. Technol.,* Vol 19, 2003, p 987
48. N. Ali, G. Cabral, A.B. Lopes, and J. Gracio, *Diamond Relat. Mater.,* Vol 13 (No. 3), 2004, p 494
49. N. Ali, Q.H. Fan, W. Ahmed, and J. Gracio, *Thin Solid Films,* Vol 420-421, 2002, p 155
50. S.H. Seo, T.H. Lee, and J.S. Park, *Diamond Relat. Mater.,* Vol 12, 2003, p 1670
51. M.H. Nazaré and A.J. Neves, Ed., *Properties, Growth and Applications of Diamond,* INSPEC, The Institution of Electrical Engineers, London, U.K., B2. Vol 2, 2001, p 303
52. P.N. Barnes and R.L.C. Wu, *Appl. Phys. Lett.,* Vol 62, 1993, p 37
53. T.P. Ong, F. Xiong, R.P.H. Chang, and C.W. White, *J. Mater. Res.,* Vol 7, 1992, p 2429
54. W.R.L. Lambrecht, C.H. Lee, B. Segall, and J.C. Angus, *Nature,* Vol 364, 1993, p 607
55. J. Singh, *J. Mater. Sci.,* Vol 29, 1994, p 2761